Original paper

Dose uncertainty due to needle-tip localization error in prostate seed implantation

Zhengzheng Xu, PhD[1,2], Theodore H. Arsenault, MS[1], Bryan Traughber, MD[3], Roger Ove, MD, PhD[1], Tarun K. Podder, PhD[1]

[1]Department of Radiation Oncology, Seidman Cancer Center, University Hospitals Cleveland Medical Center, Case Western Reserve University School of Medicine, Cleveland, OH 44106, USA, [2]Department of Radiation Oncology, University of Southern California, Norris Cancer Hospital, Los Angeles, CA 90033, USA, [3]Department of Radiation Oncology, Pennsylvania State University, Hershey, PA 17033, USA

Abstract

Purpose: This study quantified the dosimetric uncertainty caused by needle-tip detection errors in ultrasound images due to bevel-tip orientation differences, with respect to the location on template grid.

Material and methods: Trans-rectal ultrasound (TRUS) system with physical template grid and 18-gauge bevel-tip brachytherapy needles were used. TRUS was set at 6.5 MHz in water phantom, and measurements were taken with 50% and 100% B-mode TRUS gains. Needle-tip localization errors were then retrospectively applied back to 45 prostate seed implant plans to evaluate the important planning parameters for the prostate (D_{90}, V_{100}, V_{150}, and V_{200}), urethra (D_{10} and D_{30}), and rectum (V_{100}, D_{2cc}, and $D_{0.1cc}$), following the ABS and AAPM TG-137 guidelines.

Results: The needle-tip detection errors for 50% and 100% TRUS gains were 3.7 mm (max) and 5.2 mm (max), respectively. The observed significant decrease in prostate coverage (mean D_{90} lower by 12.8%, and V_{100} lower by 3.9% for smaller prostates) after seed placements were corrected by compensating the needle-tip detection errors. Apex of the prostate was hotter, and the base was cooler. Dosimetric difference for urethral and rectal parameters were not statistically significant.

Conclusions: This study revealed that the beveled needle-tip orientation could considerably impact the needle tips detection accuracy, based on which the seeds might be delivered. These errors can lead to significant dosimetric uncertainty in prostate seed implantation.

J Contemp Brachytherapy 2022; 14, 6: 582–589
DOI: https://doi.org/10.5114/jcb.2022.123978

Key words: dose uncertainty, needle detection error, prostate seed implant.

Purpose

Trans-perineal interstitial low-dose-rate (LDR) prostate brachytherapy is one of the common modalities of treating low- and intermediate-risk prostate cancer patients. Accurate implantation of radioactive seeds is very important for effective delivery of radiation to the prostate, with sufficient dose sparing to organs at risk (OARs).

Prostate seed implantation (PSI) is commonly performed under the guidance of trans-rectal ultrasound (TRUS), and seeds are delivered using bevel-tip needles. However, needle-tip localization difference may occur due to the ultrasound system setting (e.g., imaging orientation and ultrasound gain), bevel-tip orientation, and elevation beamwidth (side-lobe) artifacts [1, 2]. Seed placement uncertainty is affected by the ultrasound image quality, needle placement accuracy, prostate motion, and prostate edema [3-5]. It is difficult to capture this systematic error caused by ultrasound artifacts relying on TRUS for needle guidance. In addition, the deviation in seed delivery location due to the localization error of the bevel-tip needle may be responsible for the dose of the prostate to shift systematically towards the apex, and thereby, under-dosing the base of the prostate.

The dosimetric impacts of seed migration have been reported by several studies. Detrimental effects of seed migration were more severe in terms of increasing the dose to normal structures, such as rectum V_{50} may be 70% higher and urethra V_{100} may be 50% higher in the case of 6 mm migration [6]. Bues *et al*. applied stochastic three-dimensional Gaussian errors to the seeds in PSI plans. They reported acceptable (less than 5%) target coverage (e.g., D_{90}) variation, with less than 2 mm seed placement uncertainty [7]. Su *et al*. reported similar results on the impact of seed position uncertainty on D_{90} [4]. Moreover, they stated that the increased use of number of seeds was associated with less variability in dosimetry. For example, a plan using 80 seeds with 3 mm seed uncertainty demonstrated the same changes in D_{90} compared with the one using 120 seeds with 5 mm seed location uncertainty. Seed location uncertainty can affect PSI do-

Address for correspondence: Prof. Tarun K. Podder, PhD, Department of Radiation Oncology, University Hospitals Seidman Cancer Center, Case Western Reserve University School of Medicine, 11100 Euclid Avenue, Cleveland, OH 44106, USA, phone: +01-216-630-6558, e-mail: Tarun.Podder@case.edu

Received: 25.09.2022
Accepted: 16.12.2022
Published: 30.12.2022

simetry differently based on the prostate volumes, since the required number of seed is dependent on the size of the prostate as well as the anatomical distance of OARs may also vary from one patient to another. Although the increased number of seeds improves the overall dose delivery robustness, it would result in higher susceptibility to systematic positioning errors.

The needle placement accuracy depends on the quality of image, physical property of the needle (e.g., needle-tip shape, gauge), and tissue deformation, which contribute to seed placement uncertainty [1, 8]. Wan *et al*. reported the correlation between needle placement in the template and the corresponding error due to needle deflection or bending in ultrasound image; however, they did not evaluate any dosimetric uncertainty [8]. Nath *et al*. stated that the displacement between a needle image and its' planned grid point at the base of prostate should be less than 5 mm in order to keep the reduction in minimum target dose deviation less than 5% [9]. Datla *et al*. applied a model to predict the bevel-tip deflection for real-time dose monitoring during PSI [10]. Zheng and Todor have reported a novel method for accurate identification of needle-tip in TRUS images for HDR [11], where the average accuracy was 0.7 mm in water phantom. Multiple reports on dosimetric uncertainty due to needle-tip identification error for high-dose-rate (HDR) prostate brachytherapy are available in literature [12, 13]. However, dosimetric uncertainty of needle-tip detection error in PSI has not been studied adequately. Normally, it is observed in post-PSI dosimetric analysis that the base of the prostate is lightly covered and the apex becomes hotter, as compared with pre-op or intra-op plan, due to a number of reasons, such as seed or strand movement (follows the needle or stylet when retracted), uncompressing or relaxation of the prostate after needle withdrawal, inaccurate identification of needle-tip and seed deposition, etc. Any individual seed location can be adjusted when free seeds are delivered using Mick applicator, and with modern US image guidance, the actual location of an individual seed can be detected for real-time dosimetry. However, this is not possible when a seed strand (2-6 seeds held together) is delivered using a pre-loaded needle, i.e. the location of the first seed will determine the relative location of the rest of seeds in the strand; no individual seed can be adjusted. In our PSI procedure, we use pre-loaded needles, where the seeds are loaded in the needles based on the pre-operative plan created using TRUS images by setting the patient same as that would be in the operating condition on the day of the actual PSI procedure (2-4 weeks later). On the day of the procedure, in the operating room (OR), the patient is positioned exactly at the same pre-operative condition and TRUS images are acquired. The pre-op plan is then transferred to the intra-op images, and the dosimetric plan and parameters are checked before implanting the seeds by using the pre-loaded needles. The seed strand in a needle is delivered based on the location of the tip of the needle visualized in real-time TRUS image. Hence, the needle-tip detection error described in this study can result in systematic unintended seed placement deviation. In this technique (pre-loaded needle), the seed implantation is primarily determined by visualization of the needle-tip on TRUS image; therefore, the seed implantation will always be affected by the needle-tip detection error, which can further amplify due to the bevel-tip orientation. In this study, we evaluated the needle detection errors in detail for PSI, when bevel-tip needles were used. This information will be helpful for the clinicians to be aware of potential errors and related dosimetric effects, especially when using pre-loaded bevel-tip needles. During PSI procedure, the bevel-tip needle orientation can be monitored in TRUS images, and the needle-tip can be accurately identified to reduce the undesired dosimetric deviation. The purpose of this study was to evaluate the dosimetric uncertainty due to bevel-tip needle detection errors caused by variation in needle-tip orientation.

Material and methods

Imaging guidance with TRUS and QA protocol

The present study was performed with an IRB-approved protocol (STUDY# 20210259), and it was conducted using a TRUS unit (Flex Focus 500 with biplane 8848 probe, BK Medical, Burlington, MA, USA) with 6.5 MHz. The axial TRUS image combined with the virtual template grid was applied to ensure the location of the needle agrees with the physical template. Then, the longitudinal view was used to ensure the needle insertion depth. PSI treatment plans were generated using MIM Symphony version 14.4 (MIM Software Inc., Beachwood, OH, USA). Quality control for the TRUS system was performed following the American Association of Physicists in Medicine (AAPM) Task Group-128 report [14]. As the velocity of sound is the critical consideration for the ultrasound imaging and accurate detection of the needle mimicking the realistic PSI condition, a water bath phantom with a temperature at about 40°C was used for measurements. Although the recommended water temperature of 48°C would produce the same velocity of sound in soft tissue (about 1,540 m/s), the water bath temperature for the ultrasound system calibration and the experiment was kept at 40°C to have the velocity of sound closer to that in the soft tissue, and to avoid the risk of damaging the transducer.

Evaluation of needle localization error

In this study, the main focus was the errors in insertion depth caused by 18-gauge bevel-tip (20-deg beveled angle, Bard Medical, Covington, GA, USA) needle's orientation. The bevel-tip side facing away from the transducer was considered as 'beveled up' or 'tip0°', while the bevel-tip facing towards the transducer was labeled as 'beveled down' or 'tip180°'. Measurements with tip0° were considered as the reference (Figure 1A, B). Needles in the tip0° orientation (Figure 1A) were placed through PSI template grid holes (Figure 1C, D) until the needle-tip was detected on the transverse image of TRUS. A clamp was used to keep the needle in place to assist depth measurement (Figure 1D). Once the needle-tip was detected in TRUS image, both ultrasound probe and clamped needle were carefully removed from the water phantom

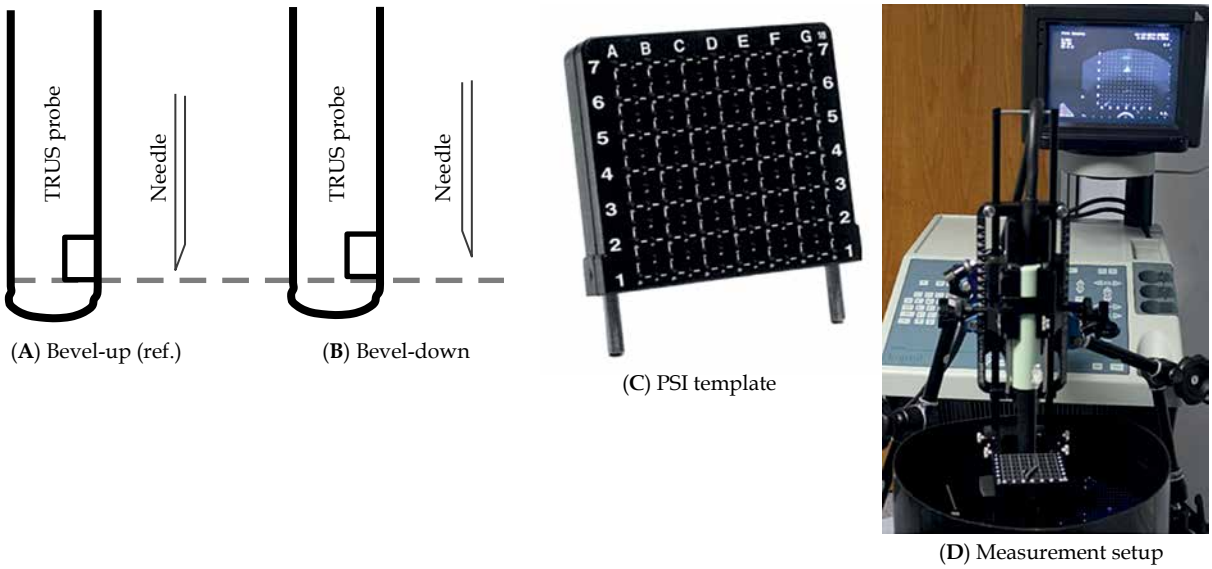

(**A**) Bevel-up (ref.) (**B**) Bevel-down (**C**) PSI template (**D**) Measurement setup

Fig. 1. Bevel-tip needle orientation with respect to trans-rectal ultrasound (TRUS) probe and measurement setup. **A**) Facing-up, i.e. beveled angle away from TRUS (reference configuration), **B**) facing down, i.e. beveled angle toward TRUS, **C**) prostate seed implantation (PSI) template grid, and **D**) experimental setup

for physical measurement and confirmation. A high-resolution digital Vernier caliper was applied to measure the needle depth in water from the template grid to the needle-tip. The needle was then rotated to tip180° (Figure 1B), and the depth was adjusted until the needle-tip appeared again in TRUS image. The depth of tip180° was then measured and compared to tip0°, this difference was the resultant 'error' solely due to opposite orientations of the bevel-tip needle. The measurements were performed for half of the template grid from columns 'a' to 'D' due to template symmetry (Figure 1C). Measurements for the axial depth ranged from 50 to 100 mm. All the measurements were acquired with 50% and 100% B-mode TRUS gains, and each measurement was repeated five times.

Dosimetric uncertainty due to needle-tip detection errors

The systematic error of needle-tip detection was retrospectively applied to a total of forty-five PSI cases performed in our clinic (monotherapy of 145 Gy with iodine-125 [^{125}I], seed model TheraSeed AgX100, Theragenics Corp., Buford, GA, USA). We took the clinical intra-op plan for each of PSI cases and seeds were moved towards the prostate apex by the amount of needle-tip errors based on the seed location, i.e., xy-coordinates or row-column number on the template's grid hole. The average seeds activity was 0.375 mCi (air-kerma strength of 0.476 U). Cases were divided into three groups in terms of prostate volume: 1) Small volume: less than 30 cm^3; 2) Medium volume: 30 to 40 cm^3; 3) Large volume: larger than 40 cm^3. Each of these groups had fifteen patients.

For each PSI case, three treatment plans were generated. 1) Plan$_{ref}$: a reference plan, which was generated during the PSI procedure and clinically accepted (i.e., intra-operative plan); 2) Plan$_{50}$: a plan with bevel-tip needle errors applied with 50% B-mode ultrasound gain; and 3) Plan$_{100}$: a plan with bevel-tip needle errors applied with 100% B-mode ultrasound gain.

Clinical intra-operative plans were generated using modified peripheral loading technique. Prostate and OARs were contoured by the physicians on TRUS images. For the intra-operative plans, prostate V_{100} > 98% was used as the minimum coverage criteria, and all the other planning criteria for the prostate (D_{90}, V_{150}, V_{200}), urethra (D_{10}, D_{30}), and rectum (V_{100}, D_{2cc}, $D_{0.1cc}$) followed the AAPM TG-137 recommendations [15].

For plans with needle localization errors (i.e., plan$_{50}$ and plan$_{100}$), an in-house MATLAB program was developed to apply needle localization errors to three-dimensional coordinates of the seeds in DICOM plan files. These plans were not re-optimized, only the tip detection errors were applied to the clinical intra-op plan. DICOM files were then imported back into TPS for dose calculation and DVH parameters evaluation. DVH parameters derived from plan$_{50}$ and plan$_{100}$ were compared to those from plan$_{ref}$. Statistical significance of each DVH parameter was analyzed using two-tailed Student's *t*-test, and *p*-values less than 5% were considered significant.

Results

Evaluation of needle localization error

A grid template-specific two-dimensional lookup table for the distance from transducer vs. average needle depth error was created and applied to the clinically approved intra-operative PSI plans. For 50% gain, bevel-tip detection errors of column 'a' ranged from 0.69 ±0.31 mm (1st row) to 2.75 ±0.05 mm (9th row, marked 5 on template, see Figure 1C), while those of column 'D' ranged from 0.78 ±0.31 mm (1st row) to 3.73 ±0.51 mm (9th row, marked 5 on template). For 100% gain, errors of column 'a' ranged from 0.57 ±0.25 mm (1st row) to 5.24 ±0.36 mm (9th row,

marked 5 on template), while those of column 'D' ranged from 0.84 ±0.30 mm (1st row) to 4.2 ±0.20 mm (9th row, marked 5 on template) (Figure 2).

Dosimetric uncertainty due to needle-tip detection errors

The prostate volumes ranged from 16.6 to 59.6 cm^3. The differences in DVH parameters among $plan_{ref}$, $plan_{50}$, and $plan_{100}$ are presented in Tables 1-3; a DVH plot of a representative case is presented in Figure 3. The prostate V_{100} of $plan_{50}$ demonstrated an average decreases of 3.9% ($p < 0.05$), 2.0% ($p < 0.05$), and 2.0% ($p < 0.05$) for small, medium, and large volume prostates, respectively. The decrease in V_{100} ranged from 0.5% (prostate volume of 40.8 cm^3) to 8.9% (prostate volume of 26.7 cm^3). An average deceases in D_{90} were 12.8 Gy ($p < 0.05$), 5.0 Gy ($p < 0.05$), and 5.4 Gy for small, medium, and large prostate volumes, respectively. Decreases in D_{90} varied from 1.3 Gy (prostate volume of 40.8 cm^3) to 27.0 Gy (prostate volume of 26.7 cm^3). Urethral doses deviations from reference plans ranged from 1 to 3.6 Gy for D_{30}, and 1.2 to 3.4 Gy for D_{10}, but these were not statistically significant. Similarly, rectal doses variations in planned parameters were small and were not found to be statistically significant (Tables 1-3).

Compared to the V_{100} of $plan_{50}$, the V_{100} of $plan_{100}$ exhibited larger average decreases of 4.5% ($p < 0.05$), 2.4% ($p < 0.05$), and 2.4% ($p < 0.05$) for small, medium, and large volume sizes, respectively. In addition, average decrease in D_{90} of $plan_{100}$ were larger: 6.0 Gy ($p < 0.05$) and 6.4 Gy for medium and large prostate volumes, respectively. Small and comparable rectal dose differences were observed as in the plans with TRUS gains of 50% and 100%.

Discussion

Higher B-mode ultrasound gain (100% vs. 50%) demonstrated larger DVH differences that resulted from the bevel-tip needle detection errors. The ultrasound gain difference did not have significant impact on the needle

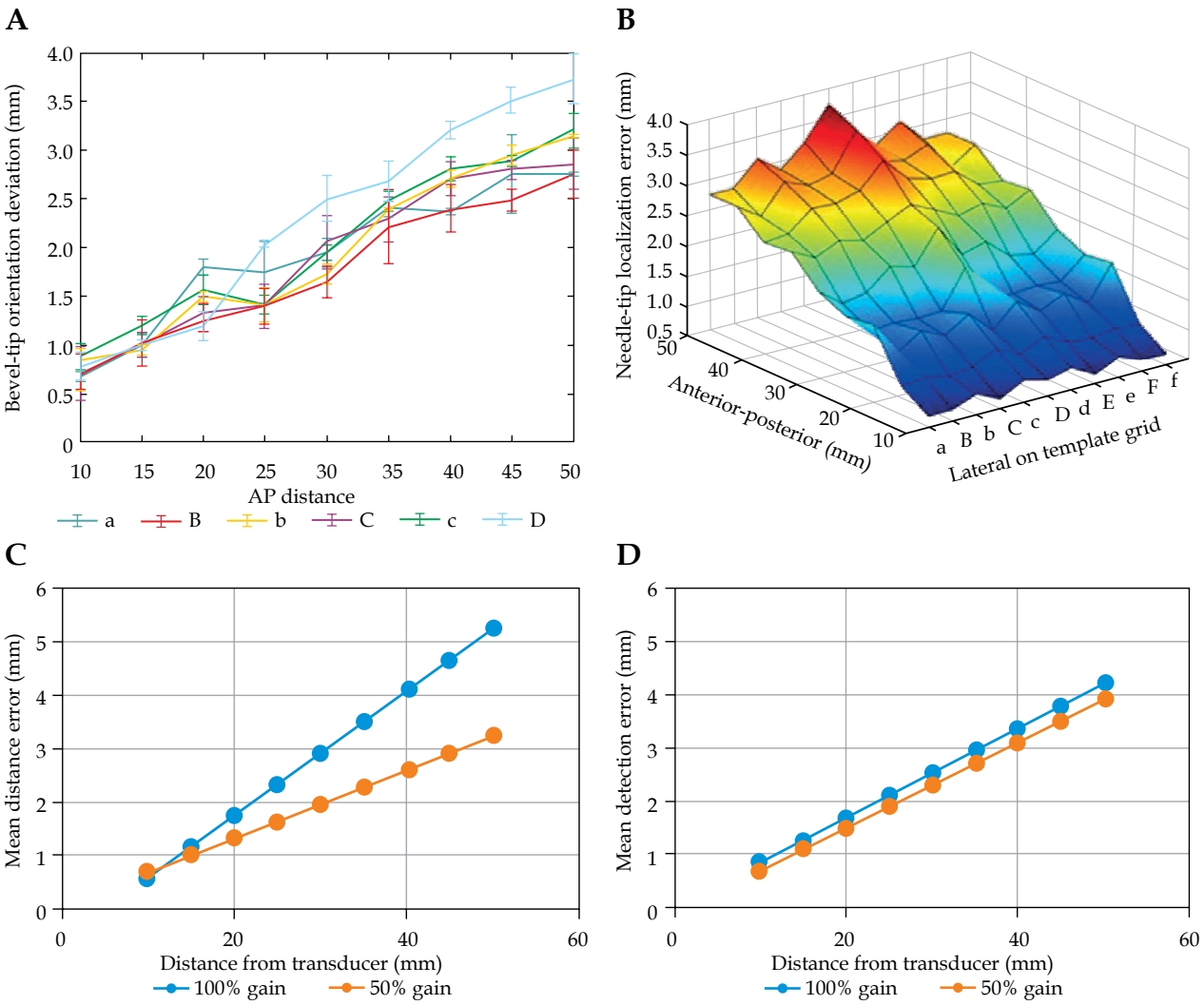

Fig. 2. Mean detection error for needle-tip position: **A, B**) With a 50% B-mode ultrasound gain setting for each lateral locations ('a' through 'D') on the prostate seed implantation (PSI) template grid, **C**) errors at 'a' column for 50% and 100% B-mode ultrasound gains, and **D**) errors at 'D' column for 50% and 100% B-mode ultrasound gains

detection error along column 'D' (Figure 2D), whereas the difference in error increased as the needle was placed away from the central column (away from vertically above TRUS transducer, Figure 2C). These results agree with the conclusion of a study conducted by Peikari *et al*. [1]. As the needle is placed away from the transducer, the ultrasound wave reflections increase, thus echoed signal from the needle-tip is reduced (Figure 4). Due to the position of the needle in relation to the transducer, the sound wave attenuates more when moving from midline to lateral position. The difference in intensity as a function of position was plotted using the following equation (1).

$$relative\ intensity\ (dB) = 10 \log\left(\frac{I_{echo}}{I_{incedent}}\right)$$
$$\text{or } \frac{I_{echo}}{I_{incedent}} = 10^{-\frac{dB}{10}} \quad (1)$$

With equation (1) and using a 6.5 MHz ultrasound beam with the assumption that there is 100% reflection between the tissue and needle interface, we can examine the differences in echo intensities at the transducer normalized to the incident intensity (Figure 4). In reality, these values will be even lower due to acoustic reflection losses, refraction, and scattering of the ultrasound wave as it traverses the medium. These losses of intensity may attribute to the deviations in needle-tip positioning, especially when moving laterally from midline (i.e., away from vertically up).

When the sound wave interacts with the needle-tip oriented towards the transducer, the curvature of the tip allows a majority of the sound wave to reflect back towards the transducer (Figure 5A). Therefore, a better physical design of the needle-tip is a solution to improve

Table 1. Dosimetric comparison of $plan_{50}$ and $plan_{100}$ with $plan_{ref}$ for patients with prostate volumes less than 30 cc

Dosimetric parameters for group 1: Small prostate (< 30 cc)						
	With 50% gain			With 100% gain		
	Mean difference	Range	*p*-value	Mean difference	Range	*p*-value
Prostate						
V_{100} (%)	–3.92 ±2.09	(–8.86, –1.39)	< 0.001	–4.51 ±2.77	(–12.11, –2.11)	< 0.001
V_{150} (%)	–3.67 ±1.85	(–6.97, –1.08)	0.443	–4.50 ±1.84	(–7.28, –1.49)	0.029
V_{200} (%)	–5.24 ±1.45	(–7.46, –2.79)	0.004	–5.50 ±1.61	(–7.95, –2.57)	0.003
D_{90} (Gy)	–12.80 ±2.11	(–27.04, –2.59)	0.001	–12.52 ±7.86	(–34.40, –5.16)	< 0.001
Prostatic urethra						
D_{30} (Gy)	3.58 ±2.26	(0.71, 7.33)	0.932	–0.10 ±3.60	(–6.26, 6.22)	0.972
D_{10} (Gy)	3.44 ±3.21	(0.17, 11.29)	0.899	0.31 ±5.21	(–6.77, 16.95)	0.928
Rectum						
V_{100} (%)	0.07 ±0.09	(0.00, 0.34)	0.867	0.03 ±0.12	(–0.17, 0.28)	0.914
D_{2cc} (Gy)	0.93 ±0.75	(0.15, 2.89)	0.930	0.63 ±1.35	(–1.34, 3.60)	0.930
$D_{0.1cc}$ (Gy)	2.64 ±2.32	(0.01, 8.18)	0.807	2.18 ±3.13	(–2.38, 9.57)	0.825

Table 2. Dosimetric comparison of $plan_{50}$ and $plan_{100}$ with $plan_{ref}$ for patients with prostate volumes between 30 and 40 cc

Dosimetric parameters for group 2: Medium prostate (30-40 cc)						
	With 50% gain			With 100% gain		
	Mean difference	Range	*p*-value	Mean difference	Range	*p*-value
Prostate						
V_{100} (%)	–2.08 ±0.87	(–3.27, 0.72)	< 0.001	–2.35 ±1.88	(–4.53, –0.43)	< 0.001
V_{150} (%)	–1.09 ±2.79	(–3.90, 8.05)	0.482	–2.70 ±1.47	(–4.87, –0.33)	0.063
V_{200} (%)	–2.87 ±2.43	(–5.71, 5.07)	0.105	–3.89 ±1.06	(–5.96, –2.15)	0.025
D_{90} (Gy)	–4.96 ±2.96	(–10.14, 1.37)	< 0.001	–6.09 ±3.96	(–12.88, –0.31)	< 0.001
Prostatic urethra						
D_{30} (Gy)	2.51 ±3.33	(0.02, 13.41)	0.876	–0.78 ±2.79	(–5.15, 4.69)	0.750
D_{10} (Gy)	2.53 ±3.25	(0.09, 13.69)	0.795	–1.59 ±3.28	(–10.65, 2.40)	0.695
Rectum						
V_{100} (%)	0.09 ±0.14	(0.00, 0.50)	0.761	0.01 ±0.11	(–0.25, 0.21)	0.966
D_{2cc} (Gy)	0.77 ±0.59	(0.04, 2.04)	0.850	0.21 ±0.74	(–1.12, 1.24)	0.953
$D_{0.1cc}$ (Gy)	1.73 ±1.52	(0.22, 5.73)	0.789	0.13 ±0.51	(–2.58, 2.93)	0.977

Table 3. Dosimetric comparison of $plan_{50}$ and $plan_{100}$ with $plan_{ref}$ for patients with prostate volumes greater than 40 cc

Dosimetric parameters for group 3: Large prostate (> 40 cc)						
	With 50% gain			With 100% gain		
	Mean difference	Range	*p*-value	Mean difference	Range	*p*-value
Prostate						
V_{100} (%)	–1.99 ±1.11	(–3.76, –0.46)	< 0.001	–2.37 ±1.22	(–4.34, –0.64)	< 0.001
V_{150} (%)	–2.46 ±1.28	(–5.44, –1.12)	0.118	–3.0 ±1.38	(–5.99, –1.00)	0.062
V_{200} (%)	–3.04 ±0.70	(–4.45, –1.98)	0.128	–3.09 ±0.71	(–4.76, –2.16)	0.119
D_{90} (Gy)	–5.40 ±2.99	(–10.84, –1.29)	< 0.001	–6.63 ±3.55	(–12.25, –1.55)	< 0.001
Prostatic urethra						
D_{30} (Gy)	1.02 ±0.97	(0.11, 3.90)	0.897	0.14 ±1.43	(–2.06, 2.69)	0.935
D_{10} (Gy)	1.24 ±0.99	(0.18, 3.27)	0.800	–0.37 ±1.50	(–3.09, 1.75)	0.807
Rectum						
V_{100} (%)	0.13 ±0.15	(0.00, 0.53)	0.689	0.07 ±0.13	(–0.15, 0.36)	0.768
D_{2cc} (Gy)	0.72 ±1.11	(–1.51, 2.79)	0.842	0.47 ±1.02	(–1.39, 2.22)	0.895
$D_{0.1cc}$ (Gy)	1.97 ±2.95	(–2.82, 8.83)	0.738	01.59 ±2.84	(–2.39, 7.91)	0.783

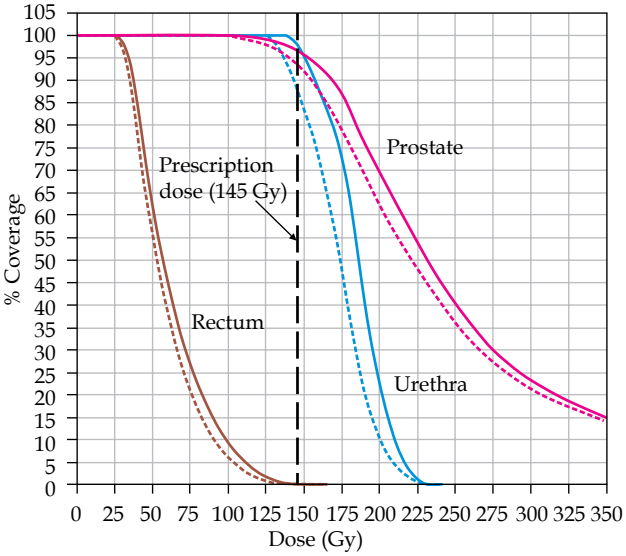

Fig. 3. Dose-volume-histogram (DVH) showing dose deviation between original plan (solid lines) and deviated plan (dotted line) for prostate (pink color), urethra (blue color), and rectum (sienna color) of a representative case. Black dashed line represents prescription dose (145 Gy)

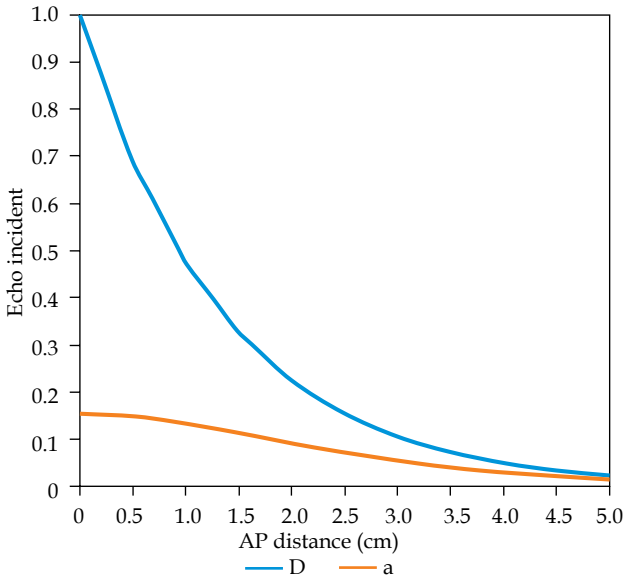

Fig. 4. Ultrasound attenuation as a function of distance from the transducer. 'D' is along the midline of the brachytherapy needle template, where 'a' is positioned the most laterally (2.5 cm)

the needle-tip detection accuracy. Wang *et al*. reported on the optimized needle designs, which can either reduce the insertion force by 11% with the same bevel length, or reduce the insertion force by 46% with an improved design [16].

Moreover, the beam width enlargement may result from an increase in the main lobe thickness, and the directed side lobe energy, which diverges further from the transducer. Needle-tip detection is more affected by the side-lobe artifacts as the gain increases, due to the increase in energy assigned to the side-lobe beam (Figure 6). The increase inside lobe energy amplifies the reflected intensity from needles positioned laterally from midline, which may explain the increase in needle-tip detection error at position 'a' for 100% gain.

The bevel-tip needle detection error resulted in significant decrease in D_{90} and V_{100} of prostate dose coverage. This impact on the prostate dose coverage is also dependent on the prostate volume and shape. The bevel-tip detection error has the most significant impact on prostates with volumes of less than 30 cm^3. The inaccuracy of seed placement in longitudinal direction is the primary factor for deviation in dosimetric coverage in prostates of small sizes, especially at the apex and at the base of

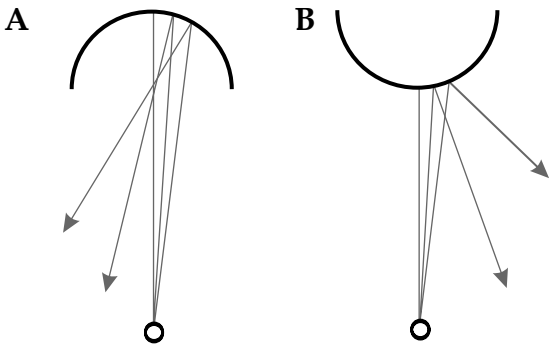

Fig. 5. Effect of needle-tip orientation on the reflected soundwave

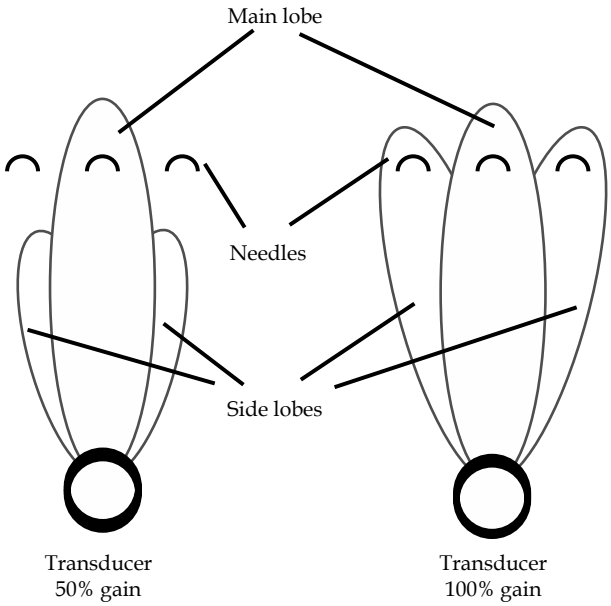

Fig. 6. As the gain increases, the frequency remains constant, while the energy assigned to the side lobe increases as shown above

the prostate. A systematic shift of the seed-strand due to bevel-tip detection error would move the seeds towards the apex, and even could bring it out of the prostate, i.e., it would not have enough prostate tissue left in the apex direct (when seen from the base to the apex) to irradiate. At the same time, the base of the prostate would be dosimetrically under-covered, resulting in decreased D_{90} and V_{100} of the target, i.e., the prostate.

The bevel-tip detection error, for 50% gain that is normally used for PSI, decrease as the needle is placed laterally from the central axis of the ultrasound probe due to increased projected reflection area (or less slant surface) and the off-axis side-lobe echoes. As a result, needle placements for prostates with larger volumes have smaller localization errors on lateral columns, but larger errors for needles in central column. However, the opposite is true for 100% gain.

The bevel-tip needle error did not have statistically significant impact on the DVH parameters of rectal and urethral doses. However, a large variation in DVH parameter changes should not be neglected. For example, the D_{2cc} and $D_{0.1cc}$ of the rectum showed an increase across the three prostate size groups for both 50% and 100% gains. When the anterior rectal wall is close to the prostate, the dose to the rectum may increase if the seeds are deposited adjacent to the prostate apex. Normally, the urethra is curved up at the apex and the base of the prostate. Therefore, an increase in urethral dose is expected if the urethra is curved at the apex when seeds are moved towards the apex.

In the literature, various solutions are suggested on compensating the needle deflection error. Real-time seeds registration can be performed either manually or automatically using mechanized device and with the application of artificial intelligence [17, 18]. Lehmann *et al*. developed a system with sensors for real-time needle-tip deflection estimation using the force-sensor-based model during needle insertion [19]. Podder *et al*. utilized a curvilinear technique, with curved needles that can achieve acceptable plan quality with 30% less needles, which eventually could reduce the tip detection error for the whole implant resulting in less dosimetric uncertainty [20]. However, realistic solutions that can be clinically implementable without requiring large resources are more desirable. The current study revealed the dose uncertainty and dosimetric coverage issue due to the error in detecting the tip of the beveled needle when the orientations of the bevel-tip are different. In clinical practice, the physician should be aware of these issues and should spin/rotate the needle, so that the needle-tip can appear on TRUS images correctly, and the tip identification can be accurate for depositing the seed at planned location. Dosimetric deviation can also be minimized by adjusting the reference needle depth with respect to the physical template grid, and visualizing the needle in both axial and sagittal planes prior to delivering a seed or seeds' strand.

One weakness of this study is that only ^{125}I cases were analyzed in this study. Because of the lower energy and higher dose gradient, the magnitude of seed localization uncertainty would be higher for palladium-103 (^{103}Pd) implants, and the opposite is true for cesium-131 (^{131}Cs) due to their higher energy and lower dose gradient [5]. Another drawback is that the dosimetric impact on post-implant dosimetry could not be evaluated because no clinical plan was delivered following the methodology studied here as well as the seed movement and migration would be compounded with the needle-tip detection errors.

Conclusions

The bevel-tip needle detection error evaluated in this study is affected by the ultrasound gain and the needle-tip orientation. It is found that the localization errors of bevel-tipped needles lead to significant under-coverage of the prostate (D_{90}, V_{100}). Prostates of small volume are affected the most by such errors. The dose uncertainty of OARs was not statistically significant. However, individual patient's anatomy should be considered to avoid unnecessary normal tissue irradiation and potential toxicity caused by needle-tip localization errors.

Disclosure

The authors report no conflict of interest.

References

1. Peikari M, Chen TK, Lasso A et al. Characterization of ultrasound elevation beamwidth artifacts for prostate brachytherapy needle insertion. *Med Phys* 2012; 39: 246-256.
2. Siebert FA, Hirt M, Niehoff P et al. Imaging of implant needles for real-time HDR brachytherapy prostate treatment using biplane ultrasound transducers. *Med Phys* 2009; 36: 3405-3412.
3. Roberson PL, Narayana V, McShan DL et al. Source placement error for permanent implant of the prostate. *Med Phys* 1997; 24: 251-257.
4. Su Y, Davis BJ, Furutani KM et al. Dosimetry accuracy as a function of seed localization uncertainty in permanent prostate brachytherapy: increased seed number correlates with less variability in prostate dosimetry. *Phys Med Biol* 2007; 52: 3105-3119.
5. Kirisits C, Rivard MJ, Baltas D et al. Review of clinical brachytherapy uncertainties: analysis guidelines of GEC-ESTRO and the AAPM. *Radiother Oncol* 2014; 110: 199-212.
6. Gao M, Wang J, Nag S, Gupta N. Effects of seed migration on post-implant dosimetry of prostate brachytherapy. *Med Phys* 2007; 34: 471-480.
7. Bues M, Holupka EJ, Meskell P, Kaplan ID. Effect of random seed placement error in permanent transperineal prostate seed implant. *Radiother Oncol* 2006; 79: 70-74.
8. Wan G, Wei Z, Gardi L et al. Brachytherapy needle deflection evaluation and correction. *Med Phys* 2005; 32: 902-909.
9. Nath S, Chen Z, Yue N et al. Dosimetric effects of needle divergence in prostate seed implant using and radioactive seeds. *Med Phys* 2000; 27: 1058-1066.
10. Datla NV, Konh B, Honarvar M et al. A model to predict deflection of bevel-tipped active needle advancing in soft tissue. *Med Eng Phys* 2014; 36: 285-293.
11. Zheng A, Todor DA. A novel method for accurate needle-tip identification in trans-rectal ultrasound-based high-dose-rate prostate brachytherapy. *Brachytherapy* 2011; 10: 466-473.
12. Fan J, Veltchev I, Lin T et al. Identification error in transrectal ultrasound-based high dose rate prostate brachytherapy. ASTRO 2017.
13. Schmid M, Juanita M, Crook JM et al. A phantom study to assess accuracy of needle identification in real-time planning of ultrasound-guided high-dose-rate prostate implants. *Brachytherapy* 2013; 12: 56-64.
14. Pfeiffer D, Sutlief S, Feng WZ et al. AAPM Task Group 128: quality assurance tests for prostate brachytherapy ultrasound systems. *Med Phys* 2008; 35: 5471-5489.
15. Nath R, Bice WS, Butler WM et al. AAPM recommendations on dose prescription and reporting methods for permanent interstitial brachytherapy for prostate cancer: Report of Task Group 137. *Med Phys* 2009; 36: 5310-5322.
16. Wang Y, Chen RK, Tai BL et al. Optimal needle design for minimal insertion force and bevel length. *Med Eng Phys* 2014; 36: 1093-1100.
17. Golshan M, Karimi D, Mahdavi S et al. Automatic detection of brachytherapy seeds in 3D ultrasound images using a convolutional neural network. *Phys Med Biol* 2020; 65: 035016.
18. Younes H, Troccaz J, Voros S. Machine learning and registration for automatic seed localization in 3D US images for prostate brachytherapy. *Med Phys* 2021; 48: 1144-1156.
19. Lehmann T, Tavakoli M, Usmani N, Sloboda R. Force-sensor-based estimation of needle-tip deflection in brachytherapy. *J Sensors* 2013; 2013.
20. Podder TK, Dicker AP, Hutapea P et al. A novel curvilinear approach for prostate seed implantation. *Med Phys* 2012; 39: 1887-1992.